Effects of Strong Color Fields on Baryon Dynamics

Sven Soff[1], Jørgen Randrup[1], Horst Stöcker[2], and Nu Xu[1]
[1] *Lawrence Berkeley National Laboratory, Nuclear Science Division 70-319, 1 Cyclotron Road, Berkeley, CA 94720, U.S.A.*
[2] *Institut für Theoretische Physik, J.W. Goethe-Universität, 60054 Frankfurt am Main, Germany*
(April 12, 2005)

arXiv:nucl-th/0209093 v2 20 Dec 2002

We calculate the antibaryon-to-baryon ratios, $\overline{p}/p, \overline{\Lambda}/\Lambda, \overline{\Xi}/\Xi$, and $\overline{\Omega}/\Omega$ for Au+Au collisions at RHIC ($\sqrt{s}_{NN} = 200\,\mathrm{GeV}$). The effects of strong color fields associated with an enhanced strangeness and diquark production probability and with an effective decrease of formation times are investigated. Antibaryon-to-baryon ratios increase with the color field strength. The ratios also increase with the strangeness content $|S|$. The netbaryon number at midrapidity considerably increases with the color field strength while the netproton number remains roughly the same. This shows that the enhanced baryon transport involves a conversion into the hyperon sector (*hyperonization*) which can be observed in the $(\Lambda - \overline{\Lambda})/(p - \overline{p})$ ratio.

Ultrarelativistic heavy ion collisions provide a unique tool to study elementary matter at energy densities so high that a phase transition from partonic deconfined matter to hadronic matter is predicted by QCD lattice calculations. The properties of such a highly excited state depend strongly on the initial conditions such as the specific entropy density or the thermalization time. A quantum number of utmost interest is the baryon number which, prior to the collision, is non-vanishing only at beam and target rapidities which for energies at the Relativistic Heavy Ion Collider (RHIC) (center-of-mass energy per nucleon-nucleon collision $\sqrt{s}_{NN} \sim 200\,\mathrm{GeV}$, Au+Au) are separated by

$$\Delta y \sim 11$$

units. Accordingly, one often assumes complete transparency, i.e., vanishing netbaryon number and $\overline{B}/B$-ratios identical with one at midrapidity. Recent data by the STAR [1], PHOBOS [2], BRAHMS [3], and PHENIX [4] collaborations, however, show that the midrapidity region $y \sim 0$ obtains a considerable finite netproton $(p - \overline{p})$ number in the final state. Moreover, the antibaryon-to-baryon ratios are not yet equal to one. The $\overline{p}/p$-ratio is about 0.7 for the most central collisions. Furthermore, rapidity spectra seem to exhibit rather a plateau than a minimum at midrapidity and large elliptic flow values indicate the need for a large amount of momentum equilibration at midrapidity providing additional evidence for a non-transparent scenario.

This strong baryon number transport over more than 5 units in rapidity is a novel phenomenon and its underlying mechanism is of utmost interest [5–9]. It also has a strong impact on other questions like the (parton) equilibration [10], the equilibration in terms of hadronic yields [11] and the build up of collective flow [12].

In this Letter we study the effects of strong color fields on the dynamics of baryons in relativistic heavy ion collisions. We will show that strong color fields lead to an enhanced baryon-antibaryon pair production and to a strong modification of the baryon transport dynamics. This will affect the antibaryon-to-baryon ratios as well as the netproton and netbaryon rapidity distributions. Moreover, the netbaryon transport to midrapidity includes a *hyperonization*, i.e., the conversion of ordinary nonstrange baryons to baryons carrying strangeness.

The idea of strong color electric fields, i.e., of an effectively increased string tension in a densely populated colored environment of highly excited matter has been suggested already earlier. The particle formation process in hadronic collisions can be viewed as quantum tunneling of quark-antiquark and gluon pairs in the presence of a background color electric field. It is formed between two receding hadrons which are color charged by the exchange of soft gluons while colliding. In nucleus-nucleus collisions the color charges may be considerably greater than in nucleon-nucleon collisions due to the almost simultaneous interaction of several participating nucleons [13]. This leads to the formation of strong color electric fields. With increasing energy of the target and projectile the number and density of strings grows, so that they start overlapping, forming clusters, which act as new effective sources for particle production [14,15]. It has been predicted that the multiplicities of, for example, strange baryons or antibaryons should be strongly enhanced [15–18] once the color field strength grows. The abundances of (multiply) strange (anti)baryons in central Pb+Pb collisions at Cern-SPS [19], for example, can only be explained within the framework of microscopic model calculations [18] if the elementary production probability of $s\overline{s}$ pairs, which is governed in the string models [20] by the Schwinger mechanism [21] $\sim \exp(-\pi m_q^2/2\kappa)$, is considerably enhanced. This corresponds either to a dramatic enhancement of the string tension κ (from the default $\sim 1\,\mathrm{GeV/fm}$ to $3\,\mathrm{GeV/fm}$) or to quark masses m_q that are reduced from their constituent quark values to current quark values as motivated by chiral symmetry restoration [18]. In a fully analog way, $\overline{p}$ abundances can be explained since an enhanced string tension similarly leads to an increased production probability of antidiquark-diquark pairs which is needed to account for

the experimentally observed yields [22]. However, this argument, providing additional motivation, has to be reconsidered if multifusion processes [23], e.g., $5\pi \rightarrow \overline{B}B$, that are neglected in microscopic transport models based on $2 \rightarrow n$ scatterings, contribute significantly to the baryon pair production. A variation of the string tension from $\kappa = 1\,\mathrm{GeV/fm}$ to $3\,\mathrm{GeV/fm}$ increases the pair production probability of strange quarks (compared to light quarks) from $\gamma_s = P(s\overline{s})/P(q\overline{q}) = 0.37$ to 0.72. Similarly, the diquark production probability is enhanced from $\gamma_{qq} = P(qq\overline{qq})/P(q\overline{q}) = 0.093$ to 0.45. In general, heavier flavors or diquarks (Q) are suppressed according to the Schwinger formula [21] by

$$\gamma_Q = \frac{P(Q\overline{Q})}{P(q\overline{q})} = \exp\left(-\frac{\pi(m_Q^2 - m_q^2)}{2\kappa}\right). \qquad (1)$$

Additional motivation of an effectively enhanced string tension in a densely colored environment is given due to its relation to the Regge slope α'. Based on a rotational string picture the string tension κ is related to the Regge slope α' by [24,25]

$$\kappa = \frac{1}{2\pi\alpha'}. \qquad (2)$$

The empirical value of the Regge slope for baryons is $\alpha' \approx 1\,\mathrm{GeV}^{-2}$ [26] that yields a string tension of approximately $1\,\mathrm{GeV/fm}$. However, high-energetic processes dominated by Pomeron exchange, characterizing the multi-gluon exchange processes existent in high-energetic nucleus nucleus collisions, are described by a Regge trajectory (Pomeron) with a smaller slope of $\alpha'_P \approx 0.4\,\mathrm{GeV}^{-2}$ [27,28]. According to Eq. (2) this translates into a considerably larger (*effective*) string tension κ.

It has been suggested recently that the magnitude of a typical field strength at RHIC energies might be as large as $5 - 12\,\mathrm{GeV/fm}$ [29] (as a result of collective effects related to quark-gluon-plasma formation). This in turn may enhance an anti-flow component resulting in a novel wiggle structure (that in general can have different origins [29–33]) around midrapidity in semi-central collisions [29].

For our investigation of the baryon dynamics in heavy ion collisions at RHIC a microscopic transport approach based on the covariant propagation of constituent quarks and diquarks accompanied by mesonic and baryonic degrees of freedom is applied [34]. It simulates multiple interactions of ingoing and newly produced particles, the excitation and fragmentation of color strings and the formation and decay of hadronic resonances. Standard type fragmentation functions are used to assign the individual hadrons of the string break-up a longitudinal momentum fraction x. Leading nucleons obey the distributions

$$f(x)_n = \exp(-(x-b)^2/(2a^2))$$

with the maximum at $b = 0.42$ and the width $a = 0.275$. For the produced hadrons a Field-Feynman fragmentation function [35] is used

$$f(x)_p = (1/3)((1-x)^d c(d+1) + 1 - c)$$

with constants $c = 1$ and $d = 2$. At RHIC energies, subhadronic degrees of freedom are of major importance. They are treated in the Ultra-relativistic Quantum Molecular Dynamics (UrQMD) model [34] via the introduction of formation times for hadrons that are produced in the fragmentation of strings [20]. Leading hadrons of the fragmenting strings contain the valence-quarks of the original excited hadron. They are allowed to interact even during their formation time, with a reduced cross section defined by the additive quark model, thus accounting for the original valence quarks contained in that hadron [34]. Newly produced (di)quarks are not allowed to interact until they have coalesced into hadrons. Their formation times are inversely proportional to the string tension

$$t_f \sim 1/\kappa.$$

The larger the string tension the shorter and short-living are the strings with a certain total energy. The cross sections for leading quarks and diquarks are set to the (later to be formed) hadron hadron cross sections scaled down by quark counting

$$\sigma_{q(\tilde{M})h} = \sigma_{Mh}/2,\ \sigma_{qq(\tilde{B})h} = 2\sigma_{Bh}/3,\ \text{and}\ \sigma_{q(\tilde{B})h} = \sigma_{Bh}/3,$$

where, e.g., $q(\tilde{M})$ represents a quark of an still unformed meson $\tilde{M}$. In this way the overall stopping behaviour of protons in central S+S collisions at $E_{\mathrm{lab}} = 200\,A\mathrm{GeV}$ can be described reasonably [36]. The importance of the diquark dynamics, i.e., (re)scatterings based on quark model cross sections, for the stopping behavior thus becomes apparent [36,37]. These secondary scatterings are important for transporting baryon number from projectile and target rapidity closer to midrapidity. The baryon-baryon collision spectrum is largely dominated by diquark degrees of freedom [36]. Only for the very first collisions and at the later stage, lower energetic collisions involve fully formed baryons. Additional contributions arise from (single) quarks carrying baryon number after diquark breaking. The diquark breaking mechanism [38] is assigned a probability of ($\sim 10\%$).

Rather exotic mechanisms, e.g., baryon junctions [39,40], have been suggested in order to understand the baryon number transport in high energetic nucleus nucleus collisions. In this approach, baryon number is not necessarily carried by the valence quarks but may reside in a non-perturbative configuration of gluon fields.

There are other important model ingredients to the baryon dynamics, i.e., in particular to the baryon transport over several units in rapidity and the baryon-antibaryon pair production. The total and elastic baryon antibaryon cross sections at high energies ($> 5\,\mathrm{GeV/c}$) are parameterized according to

$$\sigma_{\mathrm{tot/el}}(p_{\mathrm{lab}}) = a + b p_{\mathrm{lab}}^n + c \ln^2 p_{\mathrm{lab}} + d \ln p_{\mathrm{lab}}$$

with appropriate constants a, b, c, d, and n to fit experimental data [34]. The $\overline{p}p$ annihilation cross section is parameterized as

$$\sigma_{\rm an}^{\overline{p}p}(\sqrt{s}) = \sigma_0(s_0/s)[(a^2 s_0)/((s-s_0)^2 + a^2 s_0) + b].$$

For the $\overline{p}n$ and the $\overline{B}B$ cross sections we assume

$$\sigma^{\overline{p}n}(\sqrt{s}) = \sigma^{\overline{p}p}(\sqrt{s})$$

and

$$\sigma^{\overline{B}B}(\sqrt{s}) = \nu_s \sigma^{\overline{p}p}(\sqrt{s})$$

with $\nu_s = 1$ if the baryons are both nonstrange and $\nu_s = \sigma_{\rm aqm}^{\overline{B}B}/\sigma_{\rm aqm}^{\overline{p}p}$ for baryons with $s_i \geq 1$ (anti)strange quarks, respectively. The energy-independent additive quark model cross section in units of mb, (here only used to scale the energy-dependent $\overline{B}B$ cross section), follows from

$$\sigma_{\rm tot}^{\rm aqm} = 40(2/3)^{(n_1+n_2)}(1-0.4s_1/(3-n_1))(1-0.4s_2/(3-n_2))$$

with $n_i = 1$ for mesons and $n_i = 0$ for baryons. For further details of the model we refer to [34].

The anti-baryon-to-baryon ratios at midrapidity are shown in Figure 1 as a function of the strangeness content $|S|$, both for $\kappa = 1\,\mathrm{GeV/fm}$ as well as for the strong color field scenario (SCF, $\kappa = 3\,\mathrm{GeV/fm}$).

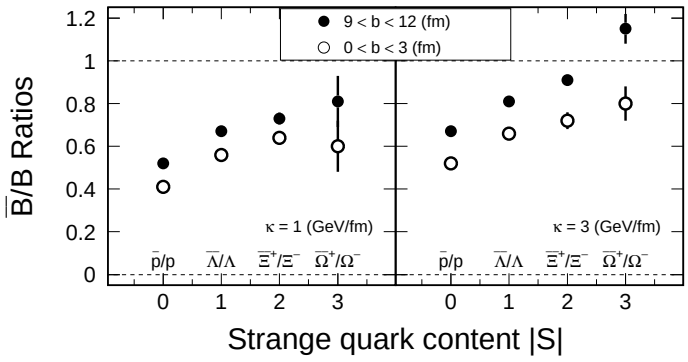

FIG. 1. Antibaryon-to-baryon ratios at midrapidity as a function of the strangeness content $|S|$ in Au+Au collisions at RHIC ($\sqrt{s}_{NN} = 200\,\mathrm{GeV}$). Calculations with a string tension of $\kappa = 1\,\mathrm{GeV/fm}$ are shown on the left and the results with strong color fields ($\kappa = 3\,\mathrm{GeV/fm}$) are shown on the right. The open and full circles correspond to rather central ($b < 3\,\mathrm{fm}$) and peripheral ($9 < b < 12\,\mathrm{fm}$) collisions, respectively.

The following systematics arise from these calculations. (i) The $\overline{B}/B$-ratios increase with the strangeness content $|S|$ of the baryons. (ii) The $\overline{B}/B$-ratios increase with impact parameter b. There is stronger absorption of antibaryons in central collisions (reducing the numerator of the ratio) and more *stopping* (increasing the denominator). (iii) Most important, the $\overline{B}/B$-ratios also increase with the color field strength κ. The dependence of the $\overline{B}/B$-ratios on κ is, a priori, not directly transparent. On the one hand, an increased pair production drives the ratio towards 1. On the other hand, reduced formation times and, hence, stronger baryon transport, reduce the ratios.

In general, the $\overline{B}/B$-ratio is determined through the pair production of $\overline{B}B$ pairs, i.e., baryons and antibaryons produced in equal amounts, and the collisions which transport (net)baryons from beam rapidity to midrapidity. Both, the pair production and the number of collisions (through smaller formation times) increase with increasing field strength κ. So in a simple ansatz one may write

$$\overline{B}/B \sim P(x)/[P(x) + C(x)],$$

where $P(x)$ is the number of produced $\overline{B}B$ pairs and $C(x)$ is the number of (net)baryons (which were transported to midrapidity). Both quantities depend on some coupling x, including the color field strength κ; (other couplings are for example the (re)absorption channels). If collisions were neglected, i.e., $C(x) = 0$, the $\overline{B}/B$-ratio equals unity. This case corresponds to (freely) decaying strings and yields the oversimplified transparency assumption as mentioned in the introduction. However, if collisions are taken into account (and this is the case in this model where the leading quarks and diquark cross sections are always nonzero, even in the formation time,) then one obtains $\overline{B}/B$-ratios smaller than unity even for small field strengths κ for which the $qq, \overline{qq}$ pair production probability is strongly suppressed (see eq. (1)). For large field strengths κ, pair production dominates resulting in larger ratios $\overline{B}/B \sim P(x)/[P(x) + C(x)] \leq 1$.

In Table I, the results for the central collisions are compared to RHIC data from STAR at $\sqrt{s} = 130\,\mathrm{GeV}$ (10% most central collisions) [41]. The results from other collaborations agree within error bars. Obviously, the calculations obtained with strong color fields agree better with the data. Note that feeddown corrections, e.g., protons from Λ decays, may further reduce the experimentally (uncorrected) ratios. Experimental error bars are statistically only.

TABLE I. $\overline{p}/p, \overline{\Lambda}/\Lambda, \overline{\Xi}/\Xi$, and $\overline{\Omega}/\Omega$ ratios at midrapidity for central Au+Au collisions at RHIC for calculations with $\kappa = 1\,\mathrm{GeV/fm}$, with strong color fields and compared to (partially preliminary) STAR data at $\sqrt{s}_{NN} = 130\,\mathrm{GeV}$.

	$\kappa = 1\,\mathrm{GeV/fm}$	(SCF) $\kappa = 3\,\mathrm{GeV/fm}$	exp. data
$\overline{p}/p$	0.41 ± 0.01	0.52 ± 0.01	0.72 ± 0.01
$\overline{\Lambda}/\Lambda$	0.56 ± 0.01	0.66 ± 0.02	0.73 ± 0.03
$\overline{\Xi}/\Xi$	0.64 ± 0.03	0.72 ± 0.04	0.83 ± 0.03
$\overline{\Omega}/\Omega$	0.60 ± 0.12	0.80 ± 0.08	0.95 ± 0.15

The rapidity spectra for netprotons ($p - \overline{p}$) and netbaryons ($B - \overline{B}$) are shown for different centralities in Figure 2. For the most central collisions, the rather strong maxima at $y \approx 3.2$ ($\kappa = 1\,\mathrm{GeV/fm}$) are weakened and shifted closer to midrapidity ($y \approx 1.8$) in the case of strong color fields ($\kappa = 3\,\mathrm{GeV/fm}$). The number of netprotons at midrapidity seems to be independent on the color field strength (≈ 12) while the number of netbaryons increases (from about 32 to 42). Hence, the larger netbaryon number at midrapidity results from strange baryons.

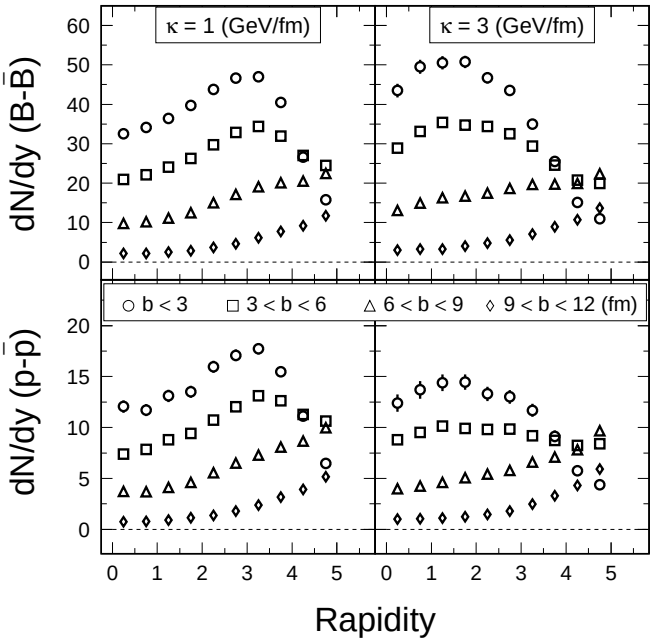

FIG. 2. Rapidity distributions for net-baryons (top) and net-protons (bottom) in Au+Au collisions at RHIC ($\sqrt{s}_{NN} = 200\,\mathrm{GeV}$). Calculations with a standard string tension ($\kappa = 1\,\mathrm{GeV/fm}$) are shown on the left and the results with strong color fields ($\kappa = 3\,\mathrm{GeV/fm}$) are shown on the right. The symbols correspond to different centralities ($b < 3\,\mathrm{fm}$ (circles), $3 < b < 6\,\mathrm{fm}$ (squares), $6 < b < 9\,\mathrm{fm}$ (triangles), and $9 < b < 12\,\mathrm{fm}$ (diamonds)).

This *hyperonization* can also be seen in the $(\Lambda - \overline{\Lambda})/(p - \overline{p})$ ratio at midrapidity which is ~ 0.45 for calculations with $\kappa = 1\,\mathrm{GeV/fm}$ and strongly enhanced ~ 0.8 for the strong color field (SCF) ($\kappa = 3\,\mathrm{GeV/fm}$) scenario, corresponding to the experimental value [4,1]. Note that Σ^0's and $\overline{\Sigma^0}$'s are included in the Λ's and $\overline{\Lambda}$'s, respectively, because they cannot be distinguished experimentally.

Another consequence of strong color fields is an increase of the pressure (gradients). This, in turn, may lead to strongly enhanced elliptic flow values as large as observed in the data. This provides a possible explanation for the lack between calculations that assume the *vacuum* string tension and that predict elliptic flow values [42] too small compared to data at RHIC [43].

The transport of other quantum numbers that can be examined in AA as well as in pA collisions include strangeness [18] and isospin [34,44]. Those can provide a complementary picture of the baryon number transport and do not need to be conserved locally.

We have calculated the antibaryon-to-baryon ratios, netbaryon and netproton rapidity distributions for Au+Au collisions at RHIC energies, and have demonstrated the important effects of strong color fields on these observables. An enhanced pair production of strange quarks and diquarks and reduced formation times lead to larger $\overline{B}/B$-ratios and to a stronger rapidity loss for the netprotons and netbaryons. More netbaryons are transported to midrapidity in the strong color field scenario which is accompanied by a hyperonization of these netbaryons. This hyperonization can be observed through an enhanced $(\Lambda - \overline{\Lambda})/(p - \overline{p})$ ratio and possibly represents the clearest signature of the flavor equilibration in relativistic heavy ion collisions.

ACKNOWLEDGMENTS

We are grateful to M. Bleicher, K. Schweda, X. N. Wang for valuable comments. We thank the UrQMD collaboration for permission to use the UrQMD transport model. S.S. has been supported by the Alexander von Humboldt Foundation through a Feodor Lynen Fellowship. This research used resources of the National Energy Research Scientific Computing Center (NERSC). This work is supported by the U.S. Department of Energy under Contract No. DE-AC03-76SF00098, the BMBF, GSI, and DFG.

[1] C. Adler *et al.* [STAR Collaboration], Phys. Rev. Lett. **87**, 262302 (2001); Phys. Rev. Lett. **86**, 4778 (2001); Phys. Rev. Lett. **89**, 092301 (2002).
[2] B. B. Back *et al.* [PHOBOS Collaboration], Phys. Rev. Lett. **87**, 102301 (2001).
[3] I. G. Bearden *et al.* [BRAHMS Collaboration], Phys. Rev. Lett. **87**, 112305 (2001).
[4] K. Adcox *et al.* [PHENIX Collaboration], Phys. Rev. Lett. **88**, 242301 (2002); Phys. Rev. Lett. **89**, 092302 (2002).
[5] W. Busza, A. S. Goldhaber, Phys. Lett. B **139**, 235 (1984); W. Busza, R. Ledoux, Ann. Rev. Nucl. Part. Sci. **38**, 119 (1988).
[6] H. Sorge, A. von Keitz, R. Mattiello, H. Stöcker, W. Greiner, Phys. Lett. B **243**, 7 (1990); T. Schönfeld *et al.*, Mod. Phys. Lett. A **8**, 2631 (1993).
[7] I. N. Mishustin, J. I. Kapusta, Phys. Rev. Lett. **88**, 112501 (2002).
[8] M. Danos, J. Rafelski, Heavy Ion Physics **14**, 97 (2001).
[9] L. Frankfurt, M. Strikman, Phys. Rev. Lett. **66**, 2289 (1991).
[10] X. N. Wang, M. Gyulassy, Phys. Rev. Lett. **68**, 1480 (1992).

[11] P. Braun-Munzinger, I. Heppe, J. Stachel, Phys. Lett. B **465**, 15 (1999).
[12] W. Scheid, H. Müller, W. Greiner, Phys. Rev. Lett. **32**, 741 (1974).
[13] K. Kajantie, T. Matsui, Phys. Lett. B **164**, 373 (1985).
[14] T. S. Biro, H. B. Nielsen, J. Knoll, Nucl. Phys. **B245**, 449 (1984). J. Knoll, Z. Phys. **C38**, 187 (1988).
[15] H. Sorge, M. Berenguer, H. Stöcker, W. Greiner, Phys. Lett. B **289**, 6 (1992). N. S. Amelin, M. A. Braun, C. Pajares, Phys. Lett. B **306**, 312 (1993). H. Sorge, Nucl. Phys. A **630**, 522 (1998).
[16] M. Gyulassy, Quark Gluon Plasma, Advanced Series on Directions in High Energy Physics, Vol. 6, edited by R. C. Hwa, World Scientific, Singapore, 1990.
[17] L. Gerland *et al.*, Proc. of the 4th International Workshop, Relativistic Aspects of Nuclear Physics, Rio, Brazil, (1995), T. Kodama et al., eds., 437.
[18] S. Soff *et al.*, Phys. Lett. B **471**, 89 (1999); S. Soff *et al.*, J. Phys. **G27**, 449 (2001).
[19] E. Andersen *et al.* [WA97 Collaboration], Phys. Lett **B433**, 209 (1998).
[20] B. Andersson, G. Gustafson, G. Ingelman, T. Sjöstrand, Phys. Rept. **97**, 31 (1983).
[21] J. S. Schwinger, Phys. Rev. **82**, 664 (1951).
[22] M. Bleicher *et al.*, Phys. Lett. B **485**, 133 (2000).
[23] R. Rapp, E. Shuryak, Phys. Rev. Lett. **86**, 2980 (2001); C. Greiner, S. Leupold, J. Phys. G **27**, L95 (2001).
[24] P. Goddard, J. Goldstone, C. Rebbi, C. B. Thorn, Nucl. Phys. B **56**, 109 (1973); K. Johnson, C. B. Thorn, Phys. Rev. D **13**, 1934 (1976).
[25] C. Y. Wong, *Introduction To High-Energy Heavy Ion Collisions*, *World Scientific, Singapore (1994), 516 p.*
[26] M. B. Green, Phys. Scripta **T15**, 7 (1987).
[27] G. Veneziano, Phys. Rept. **9**, 199 (1974).
[28] P. D. Collins, *An Introduction To Regge Theory And High-Energy Physics, Cambridge 1977, 445p.*
[29] V. Magas, L. Csernai and D. Strottman, Phys. Rev. C **64**, 014901 (2001). hep-ph/0202085.
[30] S. Soff *et al.*, Phys. Rev. C **51**, 3320 (1995).
[31] L. Csernai, D. Röhrich, Phys. Lett. B **458**, 454 (1999).
[32] R. Snellings *et al.*, Phys. Rev. Lett. **84**, 2803 (2000).
[33] J. Brachmann *et al.*, Phys. Rev. C **61**, 024909 (2000).
[34] S. A. Bass *et al.*, Prog. Part. Nucl. Phys. **41**, 255 (1998); M. Bleicher *et al.*, J. Phys. **G25**, 1859 (1999).
[35] R. Field, R. Feynman, Nucl. Phys. B **136**, 1 (1978).
[36] L. A. Winckelmann *et al.*, Nucl. Phys. A **610**, 116 (1996).
[37] M. Bleicher *et al.*, Phys. Rev. C **62**, 024904 (2000).
[38] A. Capella and B. Z. Kopeliovich, Phys. Lett. B **381**, 325 (1996); A. Capella, C. A. Salgado, Phys. Rev. C **60**, 054906 (1999).
[39] D. Kharzeev, Phys. Lett. B **378**, 238 (1996).
[40] S. E. Vance, M. Gyulassy, X. N. Wang, Phys. Lett. B **443**, 45 (1998).
[41] G. Van Buren, in Proceedings of Quark Matter 2002, Nantes, France (to be published).
[42] M. Bleicher, H. Stöcker, Phys. Lett. B **526**, 309 (2002).
[43] K. H. Ackermann *et al.* [STAR Collaboration], Phys. Rev. Lett. **86**, 402 (2001).
[44] F. Rami *et al.* [FOPI Collaboration], Phys. Rev. Lett. **84**, 1120 (2000).